

# Quantum TV and Applications in Image Processing

Jianhong (Jackie) Shen and Sung Ha Kang \*

## Abstract

Closely inspired by the Total Variation (TV) model by Rudin, Osher and Fatemi [*Physica D*, 60:259-268,1992], we propose the quantized or quantum TV model (either with a preassigned quanta set  $Q$  or without), and study the associated mathematical properties and computational algorithms. An algorithm based on stochastic or Markovian gradient descent is proposed to handle the discrete programming nature of the quantum TV model, which further leads to a two-step iterative algorithm for the computationally more challenging *free* quantum TV model. We also demonstrate several major applications of the proposed models and algorithms in bar code scanning, image quantization, and image segmentation.

## 1 Introduction

Ever since it was first introduced for image restoration by Rudin, Osher and Fatemi, total-variation (TV) based regularization [19] has found a wide range of applications in contemporary imaging and vision. Many variations of the original TV model have been proposed for further improved or extended applicability, e.g., adaptive methods proposed in [4, 5, 14], and novel applications in and links to other areas of imaging and vision [1, 5–7, 21, 24, 28], only to name a few. Recently, the importance of images with bounded variations (BV) has also been further reiterated in Meyer’s  $G$ -norm analysis for texture modeling [2, 3, 16, 18, 25, 26]. The most striking difference between classic Sobolev images and BV images lies in that BV images allow jumps or lower dimensional singular features, which are indispensable for processing images or other signals acquired in a world filled with individual objects and patterns.

A typical variational model with TV regularization has the following canonical form:

$$\min_{u \in \text{BV}} E[u | f, K] = \min_{u \in \text{BV}} \int_{\Omega} |Du| + G_{\lambda}[f|u, K], \quad (1)$$

where the first term denotes the TV Radon measure, and the second term is a suitable fidelity term ensuring that the candidate  $u$  must well “explain” a given observation  $f$ .  $\lambda$  and  $K$  are appropriate system parameters or parametric fields. For example, for image deblurring under additive Gaussian white noise, one has  $f = K * u + n$  with a point spread function (PSF)  $K$  and Gaussian noise  $n$ , and the fidelity term must be given by

$$G_{\lambda}[f | u, K] = \frac{\lambda}{2} \int_{\Omega} (f - K * u)^2 dx,$$

with  $\lambda$  inversely proportional to the variance of the noise  $\mu$ . In order to focus on the core idea of the present work, we shall assume in what follows that  $G_{\lambda}[f | u, K] = \frac{\lambda}{2} \int_{\Omega} (u - f)^2 dx$ , i.e., without any significant blur  $K$ .

In this paper, we are interested in a *quantized* or *quantum* version of the TV model (1) for which the candidate image  $u$  only takes values from a finite discrete set (the quanta set). This has been primarily motivated by a number of emerging problems in contemporary imaging and vision.

---

\*The first author is affiliated with the School of Mathematics, University of Minnesota, Minneapolis, MN 55455, USA. The second author (corresponding author) is affiliated with the Department of Mathematics, University of Kentucky, Lexington, KY 40515, USA, (skang@ms.uky.edu). The work has been partially supported by NSF (USA) under grant number DMS-0604510.

- (a) *Restorations of Binary Images.* One important example in daily life concerns the robust reading of black-white bar codes at checkout counters [10, 12, 20].
- (b) *Image Quantization.* When high fidelity images are to be displayed on low fidelity or low-bit devices (e.g., cell phones), the images needs to be properly quantized.
- (c) *Image Segmentation.* Segmentation is a central task in imaging and vision. While there are numerous remarkable segmentation models in existence with various degrees of complexity, the simplest one is perhaps just to cluster according to color shades. The piecewise constant Mumford-Shah model is such an example, by which an image is partitioned into different object patches and each object takes a specific discrete value. This can often provide very cheap but reasonably good initial guesses to more sophisticated or expensive segmentation models.

The TV model in which the candidate image  $u$  takes only a finite number of discrete values will be referred to as the *quantum TV model* in the present work. With such discrete constraints, the quantum TV model becomes a harder problem involving discrete or nonlinear programming. Classical continuum methods, such as continuous gradient-descent marching, cannot be straightforwardly applied without proper adaption or revision. Notice that while the notion of quantum TV makes perfect sense, quantum Sobolev would be less meaningful. This is a characteristic property of the TV Radon measure.

The paper is organized as follows. In Section 2, we present the proposed quantum TV model followed by discussion on the uniqueness and existence of the minimizer. In Section 3, after a brief exploration on classic (and deterministic) iterative schemes, a novel stochastic algorithm is presented to compute the quantum TV model. In Section 4, a two-step algorithm (alternating on geometric and photometric features) is proposed for the *free* quantum TV model for which the quanta set is also unknown. Generic numerical results and examples are presented in Section 5.

## 2 Quantum TV Model and Its Analysis

### 2.1 Quantum TV, Free Quantum TV, and Mumford-Shah

Let  $Q \subset \mathbb{R}$  be a nonempty finite set of real numbers. Define the  $Q$ -BV space by

$$\text{BV}^Q = \text{BV}(\Omega; Q) = \{u \in \text{BV}(\Omega) : u(x) \in Q, \text{ a.e. } x \in \Omega\}. \quad (2)$$

Here  $\Omega$  denotes a given bounded 2-D image domain, which is usually a rectangle in most digital applications. We refer to  $Q$  as the *quanta set* and assume its cardinality to be  $|Q| = k + 1$ . Since gray images are often normalized to the canonical range  $[0, 1]$ , we are particularly interested in a quanta set of the following form:

$$Q = \{0 \leq c_0 < c_1 < \dots < c_k \leq 1\}.$$

Notice that for such finite quanta set, the definition (2) makes less sense for Sobolev images since it would require the quanta set to be a singleton, and consequently the set in (2) only contains trivial constant images.

Under the constraint of the quanta set  $Q$ , the TV model (1) becomes

$$\min_{u \in \text{BV}^Q} E[u | f] = \min_{u \in \text{BV}^Q} \int_{\Omega} |Du| + \frac{\lambda}{2} \int_{\Omega} (f - u)^2 dx. \quad (3)$$

We refer to this model as a quantum TV model with a (prescribed) quanta set  $Q$ . The optimal image  $u_*$  is thus a BV function that is quantized by the quanta set  $Q$  and minimizes the TV model.

Furthermore, in some application, the specific values  $c_i$ 's of the quanta set  $Q$  cannot be predefined, except for its cardinality  $k + 1 = |Q|$ . This leads to

$$\min_{u \in \text{BV}^Q, |Q|=k+1} E[u] = \min_{u \in \text{BV}^Q, |Q|=k+1} \int_{\Omega} |Du| + \frac{\lambda}{2} \int_{\Omega} (f - u)^2 dx. \quad (4)$$

For convenience, we shall refer to it as a *free quantum TV model*.

These quantum TV models (3) and (4) can be closely related to *image segmentation*. For example, each value  $c_i$  in a quanta set  $Q$  can define a segment in a quantum image  $u$ , and a natural partitioning thus results:

$$\Omega_i = \{x \in \Omega \mid u(x) \equiv c_i\}, \quad c_i \in Q.$$

In the context of pattern and data analysis, this approach amounts to color-based pixel clustering. Pixels sharing a same color shade are partitioned into a same virtual “object.”

Recall that the piecewise constant Mumford-Shah [11, 17, 22] model for a given image  $f$  is given by

$$\min_{\Gamma} E_{MS}[\Gamma, c|f] = \mathcal{H}^1(\Gamma) + \frac{\lambda}{2} \sum_{i=1}^k \int_{\Omega_i} (f - c_i)^2 dx, \quad (5)$$

Here  $\Gamma$  denotes the partitioning boundary set with a finite 1D Hausdorff measure  $\mathcal{H}^1$ , and  $\{\Omega_i : i = 0, 1, \dots, k\}$  are the connected components of  $\Omega \setminus \Gamma$ . Implemented by the level-set method, this reduced Mumford-Shah model (5) has also been frequently referred to as the *Chan-Vese model* [8], who rediscovered the model from the viewpoint of robust active contours. Along this line, the free quantum TV model (4) can also be expressed as:

$$E[u, Q|f] = \int_{\Gamma} |[u]| ds + \frac{\lambda}{2} \sum_{i=0}^k \int_{\Omega_i} (f - c_i)^2 dx. \quad (6)$$

Here  $u \in \text{BV}^Q$  is given by

$$u = \sum_{i=0}^k c_i 1_{\Omega_i}(x), \quad \Omega \setminus \Gamma = \cup_{i=0}^k \Omega_i, \quad Q = \{c_0 < c_1 < \dots < c_k\},$$

and  $|[u]|$  denotes the (absolute) jump magnitude along  $\Gamma$ . Therefore, under the free quantum TV model, each piece  $\gamma$  of the jump set  $\Gamma$  bordering two patches  $\Omega_i$  and  $\Omega_j$  contributes a cost of  $|c_j - c_i| \mathcal{H}^1(\gamma)$ , instead of  $\mathcal{H}^1(\gamma)$  in the Mumford-Shah model. This data dependence increases the complexity of the free quantum TV model.

## 2.2 Minimizers to Quantum TV

In this section, we analyze both the existence and the uniqueness of the minimizers to the quantum TV model (3):

$$\min_{u \in \text{BV}^Q} E[u] = \min_{u \in \text{BV}^Q} \int_{\Omega} |Du| + \frac{\lambda}{2} \int_{\Omega} (f - u)^2 dx,$$

given a noisy image  $f(x) \in [0, 1]$ , and a specified finite quanta set  $Q \subset [0, 1]$ .

**Theorem 2.1 (Existence)** *For any given  $\lambda > 0$ , quanta set  $Q \subset [0, 1]$  with  $|Q| = k + 1 \geq 1$ , and any measurable image  $f$  on  $\Omega$  whose range is within  $[0, 1]$ , there exists at least one minimizer in  $\text{BV}^Q$  to the quantum TV model (3).*

*Proof.* Take any quantum datum  $c_i \in Q$  and define  $\tilde{u} \equiv c_i$  such that  $\tilde{u} \in \text{BV}^Q$ . Then  $E[\tilde{u}|f, Q] < \infty$  since  $f$  is bounded. Consequently, one must have  $\inf_{u \in \text{BV}^Q} E[u|f, Q] < +\infty$ . Let  $\{u_n\}_{n=1}^{\infty}$  be a minimizing sequence, such that

$$\inf_{u \in \text{BV}^Q} E[u|f, Q] = \lim_{n \rightarrow \infty} E[u_n|f, Q].$$

For convenience, one can assume that for some  $M > 0$ ,

$$E[u_n|f, Q] = \int_{\Omega} |Du_n| + \frac{\lambda}{2} \int_{\Omega} (u_n - f)^2 \leq M, \quad \text{for } n = 1 \dots \infty.$$

Since  $Q \subset [0, 1]$ , this implies that  $\{u_n\}$  must be a bounded sequence in  $BV(\Omega)$ . By the precompactness of a bounded BV set in  $L^1(\Omega)$ , one can select a subsequence of  $\{u_n\}$  (still denoted by  $\{u_n\}$  after relabeling for convenience), such that  $u_n \rightarrow u_*$  in  $L^1(\Omega)$  for some  $u_* \in L^1(\Omega)$ . The convergence can be further assumed to be a.e. convergence after another round of subsequence refinement and relabeling.

By the  $L^1$ -lower semi-continuity of the TV semi-norm, one has

$$\int_{\Omega} |Du_*| \leq \liminf_{n \rightarrow \infty} \int_{\Omega} |Du_n|. \quad (7)$$

By Lebesgue's Dominated Convergence (since  $\|u_n - f\|_{\infty} \leq \|u_n\|_{\infty} + \|f\|_{\infty} \leq 2$ ), one has

$$\int_{\Omega} (u_* - f)^2 = \lim_{n \rightarrow \infty} \int_{\Omega} (u_n - f)^2.$$

In combination, one has

$$E[u_*|f, Q] \leq \liminf_{n \rightarrow \infty} E[u_n|f, Q] = \inf_{u \in BV^Q} E[u|f, Q]. \quad (8)$$

Now that for a.e.  $x \in \Omega$ ,  $u_n(x) \rightarrow u_*(x)$  and  $u_n(x) \in Q$ , we conclude that a.e. for each given  $x \in \Omega$ , there must exist some index  $N_x$  and some unique  $c_x \in Q$ , such that  $\forall n > N_x$ ,  $u_n(x) \equiv c_x$ . For such a pixel, one thus must have  $u_*(x) = c_x \in Q$ . Combined with (7) or (8), this implies that  $u_* \in BV^Q$ , and that  $u_*$  is a minimizer to the quantum TV model.  $\square$

For the classical TV model (1), it is well established that the minimizer exists and is unique, since the functional is strictly convex (see, e.g., Chambolle and Lions [5]). However, this is not the case for the quantum TV model. The discrete nature of the quantum constraint  $Q$  effaces the uniqueness of the original TV restorations model. This is to be demonstrated through specific constructions as follows.

**Proposition 1** *The minimizers to the quantum TV model (3) can be non-unique.*

*Proof.* Consider the example of  $Q = \{0, 1\}$ , and  $f(x) \equiv \frac{1}{2}$ . Then, for any  $u \in BV^Q$ ,

$$E[u|f, Q] = \int_{\Omega} |Du| + \frac{\lambda}{2} \int_{\Omega} (u - f)^2 \geq \frac{\lambda}{2} \int_{\Omega} (u - f)^2 dx = \frac{\lambda}{2} \left(\frac{1}{2}\right)^2 |\Omega| = \frac{\lambda}{8} |\Omega|.$$

It is apparent that the lower bound is achieved if and only if  $\int_{\Omega} |Du| = 0$ . That is, either  $u \equiv 0$  or  $u \equiv 1$ , leading to *two* minimizers.  $\square$

**Proposition 2 (Number of Minimizers and  $\lambda$ : A 1D Construction)** *Let  $\Omega = [-1, 1]$ ,  $Q = \{0, 1\}$  and  $f = \frac{1}{4}1_{x \leq 0} + \frac{3}{4}1_{x > 0}$  as in Fig. 1 (a). Then,*

(i) *for  $\lambda > 4$ , the quantum TV model has a unique minimizer  $u(x) = 1_{x > 0}$ ;*

(ii) *for  $\lambda = 4$ , there are three minimizers; and*

(iii) *for  $\lambda < 4$ , there are two minimizers  $u \equiv 0$  and  $u \equiv 1$ .*

*Proof.*

Notice that for any  $u \in BV^Q$

$$\left(u - \frac{1}{4}\right)^2 \geq \left(\frac{1}{4}\right)^2 \wedge \left(\frac{3}{4}\right)^2 = \frac{1}{16}, \quad \left(u - \frac{3}{4}\right)^2 \geq \left(1 - \frac{3}{4}\right)^2 \wedge \left(0 - \frac{3}{4}\right)^2 = \frac{1}{16}. \quad (9)$$

Thus,

$$\frac{\lambda}{2} \int_{\Omega} (u - f)^2 dx \geq \frac{\lambda}{2} \int_{-1}^1 \frac{1}{16} dx = \frac{\lambda}{16}.$$

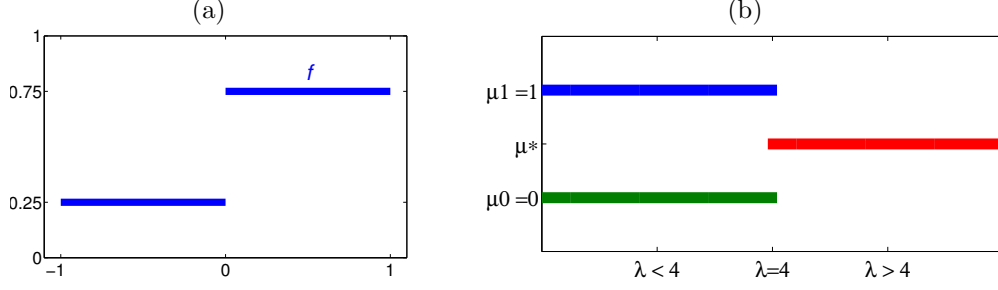


Figure 1: (a) Graph of the 1D image signal  $f$  for the non-uniqueness construction in Proposition (2). (b) Bifurcation diagram for the number of minimizers as the fitting weight  $\lambda$  varies.

The lower bound is achieved if and only if  $u = 1_{x>0} := u_*$ . Next, due to the quantum constraint  $Q$ , it is easy to see that  $TV(u) = \int_{\Omega} |Du| = 0, 1, 2, \dots$  depending on how many jumping points  $u$  has. We then consider separately three different scenarios.

(a) If  $TV(u) = 0$ , then  $u \equiv 0 := u_0$  or  $u \equiv 1 := u_1$  and both have the same energy:

$$E[u, |f, Q] = \frac{\lambda}{2} \left( \left(\frac{1}{4}\right)^2 \times 1 + \left(\frac{3}{4}\right)^2 \times 1 \right) = \frac{5\lambda}{16}.$$

(b) If  $TV(u) = 1$ , then by (9),

$$E[u|f, Q] \geq 1 + \frac{\lambda}{16},$$

and this lower bound is reached if and only if when  $u = u_* = 1_{x>0}$ .

(c) Furthermore, if  $TV[u] = j > 1$ , by (9)

$$E[u|f, Q] \geq j + \frac{\lambda}{16} > 1 + \frac{\lambda}{16}.$$

From the above three situations, it comes clear that a minimizer  $u$  of the quantum TV model must be one from  $\{u_0 \equiv 0, u_1 \equiv 1, u_* = 1_{x>0}\}$ .

When  $\lambda > 4$  (more fitting and less regularity),  $\frac{5\lambda}{16} > 1 + \frac{\lambda}{16}$ , and one must have  $\operatorname{argmin} E[u | f, Q] = u_*$ , which is unique. When  $\lambda = 4$ ,  $\frac{5\lambda}{16} = 1 + \frac{\lambda}{16}$ , and the three candidates all reach the same minimum. Finally, when  $\lambda < 4$  (more regularity and less fitting),  $\frac{5\lambda}{16} < 1 + \frac{\lambda}{16}$ , and one has  $\operatorname{argmin} E[u | f, Q] = \{u_0, u_1\}$ . This bifurcation behavior against the fitting parameter  $\lambda$  is illustrated in Fig. 1 (b).  $\square$

In subsequent sections, we explore effective algorithms that can solve the challenging discrete programming problem associated with both the quantum TV and the free quantum TV models.

### 3 Markov Gradient Descent Method for Quantum TV

To effectively compute the quantum TV model and conquer its challenging nature of discrete programming, we propose in this section a novel algorithm based on stochastic gradient descent, which amounts to a Markov random walk through the admissible space. The *stochastic* algorithm has been closely inspired by its *deterministic* predecessors based on fixed-point iteration and lagged diffusivity linearization for the TV model.

A typical fixed-point iteration can be written as

$$u^{n+1} = T(u^n), \quad n = 0, 1, \dots \quad (10)$$

The algorithm is said to be *energy decreasing* if

$$E[u^{n+1}] \leq E[u^n], \quad n = 0, 1, \dots, \infty. \quad (11)$$

The algorithm is said to be *gradient descent* in the generalized sense if

$$\int_{\Omega} \frac{\partial E[u^n]}{\partial u} \delta u^n dx \leq 0, \quad n = 0, 1, \dots, \infty, \quad (12)$$

where  $\delta u^n = u^{n+1} - u^n = T(u^n) - u^n$ .

For example, the traditional infinitesimal gradient descent scheme

$$u^{n+1} - u^n = \delta u^n = -\tau \frac{\partial E}{\partial u}[u^n],$$

if well defined, must be gradient descent in the generalized sense. Similarity, if  $E$  is strictly convex and its Hessian bilinear form  $H_n$  exists, then the Newton-Raphson iteration is also gradient descent in the generalized sense:

$$u^{n+1} = u^n - H_{u^n}^{-1} \left( \frac{\partial E}{\partial u}[u^n] \right), \quad n = 0, 1, \dots, \infty.$$

For total variation minimization, one of the well known algorithms is the lagged-diffusivity fixed point iteration (LD-FPI) [27]. Since the construction of our algorithm is closely inspired by LD-FPI, we first review some important properties of LD-FPI.

### 3.1 Review of Lagged-Diffusivity Fixed-Point Iterations(LD-FPI)

For the classical TV model (1),

$$\min_{u \in \text{BV}} E[u] = \min_{u \in \text{BV}} E[u|f] = \min_{u \in \text{BV}} \int_{\Omega} |\nabla u| dx + \frac{\lambda}{2} \int_{\Omega} (u - f)^2 dx,$$

a typical way to compute its minimizer starts from its Euler-Lagrange equation:

$$\frac{\partial E}{\partial u} = -\nabla \left( \frac{\nabla u}{|\nabla u|} \right) + \lambda(u - f), \quad (13)$$

where the first (curvature) term is understood in the distributional sense.

When one uses a direct time marching schemes

$$u^{n+1} = u^n - \Delta t \frac{\partial E[u^n]}{\partial u},$$

the CFL stability condition would demand small  $\Delta t$ . Lagged-diffusivity fixed point iteration (LD-FPI) works without the introduction of artificial time  $t$ . We refer to the excellent monograph of Vogel for more details [27]. LD-FPI is also based on the Euler-Lagrange formula (13), and is in essence a linearization technique. At each step  $n$ , given  $u^n$ , one solves  $u^{n+1}$  from

$$-\nabla \left( \frac{\nabla u^{n+1}}{|\nabla u^n|} \right) + \lambda(u^{n+1} - f) = 0$$

with Neumann boundary condition along  $\partial\Omega$ . With proper conditioning techniques, we shall assume that numerically  $u^n$  is smooth and  $|\nabla u^n| \neq 0$  (i.e., via an  $\epsilon$ -lifting  $|\nabla u|_{\epsilon} = \sqrt{|\nabla u^n|^2 + \epsilon^2}$ .) At each  $n$ , define the elliptic linear operator  $L_n = -\nabla \left( \frac{1}{|\nabla u^n|} \nabla \right)$ , then, LD-FPI becomes

$$u^{n+1} = T(u^n) := (L_n + \lambda I)^{-1}(\lambda f). \quad (14)$$

Unlike the direct time marching scheme, LD-FPI in (14) is unconditionally stable, and is more suitable for the stochastic approach proposed in this work. The two simple theorems below are important for later development.

**Theorem 3.1** *The LD-FPI scheme is energy decreasing, i.e.,  $E[u^{n+1}] \leq E[u^n]$ .*

*Proof.* Since  $L_n u^{n+1} + \lambda(u^{n+1} - f) = 0$ ,

$$\begin{aligned} u^{n+1} &= \operatorname{argmin}_z \frac{1}{2} \langle L_n z, z \rangle + \frac{\lambda}{2} \int_{\Omega} (z - f)^2 \\ &= \operatorname{argmin}_z \frac{1}{2} \int_{\Omega} \frac{1}{|\nabla u^n|} |\nabla z|^2 + \frac{\lambda}{2} \int_{\Omega} (z - f)^2 \\ &= \operatorname{argmin}_z \frac{1}{2} \int_{\Omega} \left( \frac{1}{|\nabla u^n|} |\nabla z|^2 + |\nabla u^n| \right) + \frac{\lambda}{2} \int_{\Omega} (z - f)^2. \end{aligned}$$

In the last line, we have added a constant term irrelevant to  $z$ . Let's call this functional  $G_n[z]$ , the intermediate reference energy.

Since  $u^{n+1}$  is a minimizer,

$$G_n[u^{n+1}] \leq G_n[u^n] = E[u^n] = E[u^n | f], \quad (\text{TV model (1)}).$$

By  $\frac{A+B}{2} \geq \sqrt{AB}$ , one has

$$\begin{aligned} G_n[u^{n+1}] &\geq \int_{\Omega} \left[ |\nabla u^{n+1}|^2 \frac{1}{|\nabla u^n|} |\nabla u^n| \right]^{1/2} + \frac{\lambda}{2} \int_{\Omega} (u^{n+1} - f)^2 \\ &= \int_{\Omega} |\nabla u^{n+1}| + \frac{\lambda}{2} \int_{\Omega} (u^{n+1} - f)^2 = E[u^{n+1} | f]. \end{aligned}$$

Thus,  $E[u^{n+1} | f] \leq G_n[u^{n+1}] \leq E[u^n | f]$ . □

**Theorem 3.2** *The LD-FPI scheme is gradient descent, i.e.*

$$\int_{\Omega} \frac{\partial E[u^n]}{\partial u} \delta u^n dx \leq 0, \quad \text{where } \delta u^n = u^{n+1} - u^n.$$

*Proof.* By definition,

$$\begin{aligned} \int_{\Omega} \frac{\partial E[u^n]}{\partial u} \delta u^n dx &= \int_{\Omega} \frac{\partial E[u^n]}{\partial u} (u^{n+1} - u^n) dx \\ &= \int_{\Omega} ((L_n + \lambda)u^n - \lambda f) ((L_n + \lambda)^{-1}(\lambda f) - u^n) dx \\ &= 2 \langle u^n, \lambda f \rangle - \langle (L_n + \lambda)u^n, u^n \rangle - \langle \lambda f, (L_n + \lambda)^{-1}(\lambda f) \rangle. \end{aligned}$$

On the other hand, let  $\sqrt{L_n + \lambda}$  denote the square root of the elliptic operator  $(L_n + \lambda)$ . Then, by Cauchy-Schwartz's inequality,

$$\begin{aligned} 2 \langle u^n, \lambda f \rangle &= 2 \left\langle \sqrt{(L_n + \lambda)}u^n, \sqrt{L_n + \lambda}^{-1}(\lambda f) \right\rangle \\ &\leq 2 \|\sqrt{(L_n + \lambda)}u^n\|_2 \cdot \|\sqrt{L_n + \lambda}^{-1}(\lambda f)\|_2 \\ &\leq \|\sqrt{(L_n + \lambda)}u^n\|_2^2 + \|\sqrt{L_n + \lambda}^{-1}(\lambda f)\|_2^2 \\ &= \langle (L_n + \lambda)u^n, u^n \rangle + \langle \lambda f, (L_n + \lambda)^{-1}(\lambda f) \rangle. \end{aligned}$$

Thus,  $\int_{\Omega} \frac{\partial E[u^n]}{\partial u} \delta u^n dx \leq 0$ . Furthermore, the equality holds if

$$\sqrt{(L_n + \lambda)}u^n = \sqrt{L_n + \lambda}^{-1}(\lambda f), \quad \text{or } (L_n + \lambda)u^n = \lambda f.$$

That is, if and only if  $u^n = \operatorname{argmin} E[u | f]$  is the minimizer. □

Therefore, LD-FPI is both energy diminishing and gradient descent in general sense, which will facilitate the development of our stochastic algorithm. In what follows, the operator  $T$  always refers to LD-FPI in (14).

### 3.2 Randomized gradient descent under the principle of minimum variance

Under a quantum constraint  $u \in Q$  (with  $|Q| = k + 1$ ), the LD-FPI algorithm is no longer directly applicable, since the iterative scheme  $T$  has no built-in coordination with  $Q$ . In order to still benefit from all the fine structures of LD-FPI just established above, we propose to adapt the deterministic LD-FPI  $u^{n+1} = T(u^n)$  to a stochastic setting that is applicable to the quantum TV model.

Let  $\mathbf{u}_\alpha^{n+1}$  be a random variable at a pixel  $\alpha \in \Omega$ , supported on the quanta set  $Q$ . Let  $\langle \mathbf{u}_\alpha^{n+1} \rangle$  denote its mean. Inspired by the deterministic setting above, we require the LD-FPI to still hold in the stochastic or *averaging* sense via:

$$\langle \mathbf{u}_\alpha^{n+1} \rangle = T_\alpha(u^n). \quad (15)$$

Let  $p_c$  denote the probability of  $\mathbf{u}_\alpha^{n+1} = c$  for any quantum value  $c \in Q$ :  $p_c = \text{prob}(\mathbf{u}_\alpha^{n+1} = c)$ . Then the mean is given by

$$\langle \mathbf{u}_\alpha^{n+1} \rangle = \sum_{c \in Q} cp_c.$$

Since the iteration (15) is applied from the beginning  $n = 0$ , all  $\mathbf{u}^n$ 's become random fields of (random variables). At each step  $n$ , (15) needs to be understood in the sense of conditional probability given  $\mathbf{u}^n = u^n$ , which will be indicated by a subscript  $n$ :

$$\langle \mathbf{u}_\alpha^{n+1} \rangle_n = T_\alpha(u^n), \quad \text{and} \quad \langle \mathbf{u}_\alpha^{n+1} \rangle_n = \sum_{c \in Q} cp_c. \quad (16)$$

**Proposition 3** *The stochastic LD-FPI algorithm is still gradient descent in the average sense (or in terms of conditional mean) at each step  $n$ :*

$$\left\langle \int_\Omega \frac{\partial E[u^n]}{\partial u} \delta \mathbf{u}^n dx \right\rangle_n \leq 0$$

where  $\delta \mathbf{u}^n = \mathbf{u}^{n+1} - u^n$ .

*Proof.* Since the deterministic LD-FPI iteration  $T$  is gradient descent, we have

$$\begin{aligned} \left\langle \int_\Omega \frac{\partial E[u^n]}{\partial u} \delta \mathbf{u}^n dx \right\rangle_n &= \int_\Omega \frac{\partial E[u^n]}{\partial u} \langle \delta \mathbf{u}^n \rangle_n dx \\ &= \int_\Omega \frac{\partial E(u^n)}{\partial u} (T(u^n) - u^n) dx = \int_\Omega \frac{\partial E(u^n)}{\partial u} \delta u^n dx \leq 0. \quad \square \end{aligned}$$

Thus, the gradient descent property is preserved in a stochastic sense, which will be key to energy minimization under the quantum constraint  $Q$ . However, the following proposition shows that (16) alone is insufficient to determine a unique probability distribution over a general quanta set  $Q$ .

**Proposition 4** *Unless  $Q$  is binary, i.e.  $Q = \{c_0, c_1\}$ , the mean constraint (16) is insufficient to determine the probability distribution  $(p_c)_{c \in Q}$  uniquely at each step  $n$  and for each point  $\alpha \in \Omega$ .*

*Proof.* Suppose  $\mathbf{x}$  is a random variable supported on  $Q$ , with  $p_c = \text{prob}(\mathbf{x} = c)$ , for any  $c \in Q$ . For any specified mean  $m$ , one requires:  $\sum_{c \in Q} cp_c = m$ . Also, the probability condition requires  $\sum_{c \in Q} p_c = 1$ ,  $p_c \geq 0$ , for  $c \in Q$ . Thus, when  $|Q| > 2$ , two equality constraints is not sufficient to determine  $\{p_c\}_{c \in Q}$  uniquely.  $\square$

In the deterministic setting, the gradient descent property (12) generally cannot guarantee energy decreasing in (11). The two are approximately equivalent when  $\|\delta u^{(n)}\| \ll 1$ , due to the variational principle:

$$E[u^{n+1}] - E[u^n] = \int_\Omega \frac{\partial E[u^n]}{\partial u} \delta u^n dx + \mathcal{O}(\|\delta u^n\|^2).$$

For the randomized algorithm (16), the goal is also to have the target energy steadily decreasing in some suitable stochastic sense. Therefore, we may require, on top of the mean constraint (15) or (16), that

$$\langle \|\delta \mathbf{u}^n\|^2 \rangle_n = \left\langle \int_{\Omega} (\delta \mathbf{u}^n)^2 dx \right\rangle_n \ll 1.$$

Since  $\langle \cdot \rangle_n$  commutes with  $\int \cdot dx$ , we can require more explicitly that at each pixel level  $\alpha \in \Omega$ ,

$$\langle (\delta \mathbf{u}_{\alpha}^n)^2 \rangle_n = \langle (\mathbf{u}_{\alpha}^{n+1} - u_{\alpha}^n)^2 \rangle \quad \text{is as small as possible.} \quad (17)$$

Let  $X = \mathbf{u}_{\alpha}^{n+1}$  and  $m = u_{\alpha}^n$  at each pixel  $\alpha \in \Omega$ . Assume that the sequence is close to convergence so that  $u_{\alpha}^n$  is in the close proximity of a *fixed point*  $u^*$  of the iterative scheme  $u^* = T(u^*)$ . Then one has approximately  $u^n \simeq T(u^n)$ , and the randomized algorithm (15) amounts to:

$$\langle X \rangle_n = \langle \mathbf{u}_{\alpha}^{n+1} \rangle_n = \langle T_{\alpha}(u^n) \rangle_n = u_{\alpha}^n = m.$$

Therefore,  $m$  *could* be considered as the mean value of  $X$ . Then, the requirement in (17) simply becomes

$$\text{var}(X) = \langle (X - m)^2 \rangle_n \text{ is as small as possible.}$$

We refer to this as *the Principle of Minimum Variance* (PMV).

We thus consider *the randomized gradient descent algorithm in (16) under PMV*. At each step  $n$  and a pixel  $\alpha \in \Omega$ , still denote by  $X = \mathbf{u}_{\alpha}^{n+1}$  and  $m = T_{\alpha}(u^n)$ . The probability distribution  $(p_c)_{c \in Q}$  of  $\mathbf{u}_{\alpha}^{n+1}$  is then to be determined by solving the constrained optimization problem:

$$\min_{X: \langle X \rangle = m} \text{var}(X), \quad \text{for all random variables supported on } Q. \quad (18)$$

Since  $X$  is supported on  $Q$  and  $\langle X \rangle = \sum_{c \in Q} cp_c$ , this optimization problem (18) is nontrivial if and only if  $m \in \text{conv}(Q)$ , the convex hull of  $Q$ . Otherwise, no random variable in  $Q$  can satisfy  $\langle X \rangle = m$ . For the quantum TV model targeted at image processing, we can assume that  $\{0, 1\} \subset Q$ , so that convex hull of  $Q$  is  $\text{conv}(Q) = [0, 1]$ . Then, as long as the iterative scheme  $T$  satisfies *the maximum principle*

$$\|T(u)\|_{\infty} \leq \|u\|_{\infty},$$

the above compatible condition of  $m = T_{\alpha}(u^n) \in \text{conv}(Q) = [0, 1]$  is automatically satisfied. As a result, we shall always assume  $m \in \text{conv}(Q)$  henceforth.

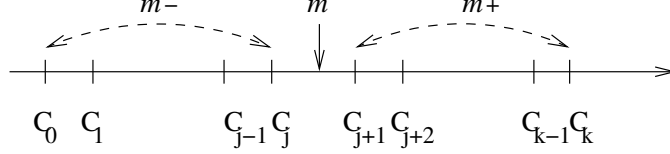
With the PMV condition, the following theorem shows that (18) has a unique solution, which resolves the earlier issue of being under-determined in Proposition 4.

**Theorem 3.3** *Suppose  $Q = \{c_0 < c_1 < \dots < c_k\}$  and  $m \in \text{conv}(Q)$ . Then, the minimization (18) has a unique solution of probability distribution  $(p_c^*)_{c \in Q}$  which is a scaled binary Bernoulli and is given as follows. Suppose  $m \in [c_j, c_{j+1}]$ , for some  $0 \leq j < k$ , then  $p_c^* \equiv 0$  for  $\forall c \notin \{c_j, c_{j+1}\}$ , and*

$$p_{c_j}^* = \frac{c_{j+1} - m}{c_{j+1} - c_j}, \quad p_{c_{j+1}}^* = \frac{m - c_j}{c_{j+1} - c_j}. \quad (19)$$

*Proof.* Consider any general distribution  $X \sim \{p_c\}_{c \in Q}$  satisfying  $\langle X \rangle = \sum_{c \in Q} cp_c = m$ . For convenience, assume  $m = 0$ . Define  $P_- = \sum_{c \in Q: c \leq c_j} p_c$  and  $P_+ = \sum_{c \in Q: c \geq c_{j+1}} p_c$ . Then  $P_- + P_+ = 1$ . Further define  $m_- = \sum_{c \in Q: c \leq c_j} c \frac{p_c}{P_-}$  and  $m_+ = \sum_{c \in Q: c \geq c_{j+1}} c \frac{p_c}{P_+}$ . Then  $P_- m_- + P_+ m_+ = m = 0$ . From these two conditions, one must have

$$P_- = \frac{m_+}{m_+ - m_-}, \quad P_+ = \frac{-m_-}{m_+ - m_-}.$$



Also notice that  $m_- \leq c_j$  and  $m_+ \geq c_{j+1}$ . Furthermore,  $m_- = c_j$  if and only if  $p_c = 0$  for all  $c < c_j$ , and  $m_+ = c_{j+1}$  if and only if  $p_c = 0$  for all  $c > c_{j+1}$ . Since we have assumed  $m = 0$  for convenience (by globally shifting  $Q$ ), we have

$$\text{var}(X) = \sum_{c \in Q} c^2 p_c = \sum_{c \leq c_j} c^2 p_c + \sum_{c \geq c_{j+1}} c^2 p_c = (v_- + m_-^2)P_- + (v_+ + m_+^2)P_+,$$

where  $v_- = \sum_{c \leq c_j} (c - m_-)^2 \frac{p_c}{P_-} \geq 0$  and  $v_+ = \sum_{c \geq c_{j+1}} (c - m_+)^2 \frac{p_c}{P_+} \geq 0$ . Thus,

$$\text{var}(X) \geq m_-^2 P_- + m_+^2 P_+ = \frac{m_-^2 m_+}{m_+ - m_-} + \frac{m_+^2 (-m_-)}{m_+ - m_-} = m_+ (-m_-) \geq c_{j+1} (-c_j).$$

Moreover, this lower bound  $c_{j+1}(-c_j)$  is reached if and only if

$$v_- = v_+ = 0, \quad \text{and} \quad m_+ = c_{j+1}, m_- = c_j (= -c_{j+1}, \text{ since } m \text{ is assumed to be } 0).$$

This lower bound corresponds to the optimal probability distribution  $p^*$  that satisfies:  $p_c^* = 0$  for all  $c < c_j$  and  $c > c_{j+1}$ , and  $p_{c_j}^* = \frac{c_{j+1} - m}{c_{j+1} - c_j}$ , and  $p_{c_{j+1}}^* = \frac{m - c_j}{c_{j+1} - c_j}$  is found.  $\square$

We are now ready to propose a stochastic algorithm for the discrete programming problem of quantum TV optimization.

### 3.3 Algorithm for Quantum TV

Based upon the above analysis, for the quantum TV model in (3),

$$\min_{u \in \text{BV}^Q} E[u] = \min_{u \in \text{BV}^Q} \int_{\Omega} |Du| + \frac{\lambda}{2} \int_{\Omega} (f - u)^2 dx,$$

we apply the LD-FPI iteration (14) via its stochastic modification in (15):

$$\langle \mathbf{u}_{\alpha}^{n+1} \rangle = T_{\alpha}(u^n).$$

Coupled with the principle of minimum variation just discussed above, this leads to unique stochastic iteration at each step, as expressed by (18).

The algorithm for quantum TV (**Algorithm 1**) is expressed as follows:

At each step  $n$  and for each pixel  $\alpha \in \Omega$ ,

**Step 1** Compute  $T_{\alpha}(u^n) := m$ .

**Step 2** Suppose  $m \in [c, d]$ , where  $c$  and  $d$  are two adjacent quanta in  $Q$ . Then, we sample  $X = \mathbf{u}_{\alpha}^{n+1}$  according to the binary Bernoulli distribution  $(c, d \mid m)$ :

$$\text{prob}(X = c) = \frac{d - m}{d - c}, \quad \text{prob}(X = d) = \frac{m - c}{d - c}. \quad (20)$$

**Step 3** Set  $u^{n+1} = X$ , and iterate to the next step.

Notice that at each step the computation goes independently at each pixel  $\alpha \in \Omega$ . Therefore, the algorithm can be easily implemented in parallel across  $\Omega$ . The key random sampling in **Step 2** can be easily realized by the following. Let  $F$  be any uniform random variable on  $[0, 1]$ . At each pixel  $\alpha \in \Omega$ , define  $T = c + (d - c)F$ . Then the random sampling by  $\mathbf{u}_\alpha^{n+1}$  can be done via:

$$\mathbf{u}_\alpha^{n+1} = \begin{cases} c, & \text{if } T > m \\ d, & \text{if } T \leq m \end{cases}. \quad (21)$$

The equivalence to (20) can be seen easily:

$$\begin{aligned} \text{prob}(\mathbf{u}_\alpha^{n+1} = d) &= \text{prob}(T \leq m) = \text{prob}(c + (d - c)T \leq m) \\ &= \text{prob}\left(T \leq \frac{m - c}{d - c}\right) = \frac{m - c}{d - c}, \end{aligned}$$

since  $T$  is uniformly distributed on  $[0, 1]$ .

**Proposition 5** *Algorithm 1 leads to a Markov Chain:*

$$\mathbf{u}^0 \rightarrow \mathbf{u}^1 \rightarrow \dots \rightarrow \mathbf{u}^n \rightarrow \mathbf{u}^{n+1} \rightarrow \dots$$

*Proof.* Recall that a random walk chain is said to be Markovian if

$$\text{prob}(\mathbf{u}^{n+1} | \mathbf{u}^n, \dots, \mathbf{u}^0) = \text{prob}(\mathbf{u}^{n+1} | \mathbf{u}^n), \quad n = 0, 1, \dots$$

This clearly holds in **Algorithm 1**, since at each step  $n$ , the distribution of  $\mathbf{u}^{n+1}$  is completely defined by  $\mathbf{u}^n$ .  $\square$

Therefore, we refer to **Algorithm 1** as *the algorithm of Markov Gradient Descent*. As shown below, it can also be understood as nearest rounding.

**Proposition 6 (Nearest Rounding and Maximum Likelihood)** *Let Algorithm 1 be modified to the following deterministic rounding, which is to be called Algorithm 2: at each step  $n$  and each pixel  $\alpha \in \Omega$ ,*

**Step 1** *compute  $m = T_\alpha(u^n)$ ; and*

**Step 2** *find the nearest  $c_* \in Q$ , such that*

$$u_\alpha^{n+1} = c_* = \text{argmin}_{c \in Q} |c - m|. \quad (22)$$

*Then, Algorithm 2 could be considered as the maximum-likelihood realization of the Markov transitions in Algorithm 1.*

*Proof.* Suppose  $m \in [c, d]$  with  $c < d$  in  $Q$ . Then

$$\text{argmin}_{c \in Q} |c - m| = \text{argmin}_{c \in \{c, d\}} |c - m|.$$

From (20),  $|c - m| \leq |d - m|$  if and only if  $\text{prob}(\mathbf{u}_\alpha^{n+1} = c) \geq \text{prob}(\mathbf{u}_\alpha^{n+1} = d)$ . Thus, the nearest-neighbor rounding (22) is equivalent to performing maximum likelihood on (20).  $\square$

## 4 The Free Quantum TV Model and Its Algorithm

In some applications such as optimal quantization and segmentation, the quanta set  $Q = \{c_j\}$  values cannot be preassigned except for its cardinality  $k + 1 = |Q|$ . This leads to a quantum TV model with a free quanta set  $Q$  (*a free quantum TV model*) as mentioned in (4) earlier:

$$\min_{u \in \text{BV}^Q, |Q|=k+1} E[u] = \min_{u \in \text{BV}^Q, |Q|=k+1} \int_\Omega |Du| + \frac{\lambda}{2} \int_\Omega (f - u)^2 dx,$$

where the quanta set  $Q$  is to be optimized as well.

Suppose  $Q = \{c_0 < c_1 < \dots < c_k\} \subset [0, 1]$  and  $u \in \text{BV}^Q$ . We define a natural image partition by  $\Omega_j = u^{-1}(c_j) = \{x \in \Omega \mid u(x) = c_j\}$ , for  $j = 0, 1, \dots, k$ . Then  $u$  can be expressed as

$$u(x) = \sum_{j=1}^k c_j 1_{\Omega_j}(x), \quad \text{a.e. } x \in \Omega.$$

As in computer graphics, we shall call  $\{c_j\}$  the *photometric feature* of  $u$  and  $\{\Omega_j\}$  the *geometric feature* of  $u$ . Thus, a quantum image  $u$  is a combination of two features, and the optimization problem (4) can be carried out by the alternating minimization (AM) technique, as well practiced in multivariate tasks in imaging and vision.

The *free quantum TV AM algorithm (AM Algorithm)* is as follows.

**G-step** (Geometric Optimization) Given  $Q$ , optimize  $u = \text{argmin}_u E[u|Q, f]$  where  $u$  is represented by the partition  $\{\Omega_j\}_{j=0}^k$ .

**P-step** (Photometric Optimization) Given  $\Omega_j$  from  $u$ , optimize the quanta set  $Q = \text{argmin}_Q E[Q|u, f]$ .

The results in Section 3 naturally applies to G-step. Thus, we shall only focus on the photometric step.

**Theorem 4.1** *Assume that each boundary  $\partial\Omega_j = \Gamma_j$  is regular enough. Define*

$$\Gamma_j^+ = \{x \in \Gamma_j \mid [u]_{\vec{\nu}} > 0\} \quad \text{and} \quad \Gamma_j^- = \{x \in \Gamma_j \mid [u]_{\vec{\nu}} < 0\},$$

where  $\vec{\nu}$  denotes the outer normal (w.r.t  $\Omega_j$ ) and

$$[u]_{\vec{\nu}} = \lim_{\epsilon \rightarrow 0^+} [u(x + \epsilon\vec{\nu}) - u(x - \epsilon\vec{\nu})], \quad \text{and} \quad \lim_{\epsilon \rightarrow 0^+} u(x - \epsilon\vec{\nu}) = c_j.$$

Then, the optimal photometric quanta set  $Q^* = \{c_j^*\}_{j=0, \dots, k}$  that minimizes the functional (6) must satisfy

$$c_j^* = \langle f \rangle_{\Omega_j} + \frac{1}{\lambda |\Omega_j|} [\mathcal{H}^1(\Gamma_j^+) - \mathcal{H}^1(\Gamma_j^-)], \quad (23)$$

for  $j = 0, \dots, k$  and  $\langle f \rangle_A = \frac{1}{|A|} \int_A f$ .

*Proof.* For a given geometric partition  $\{\Omega_i\}$ , we denote by  $F[Q]$  the free quantum TV functional in (6), to emphasize the only dependence on the quanta set  $Q$ . For each given  $j$ , the entire  $F[Q]$  can be conveniently grouped into

$$F[Q] = \int_{\Gamma_j} |[u]| ds + \frac{\lambda}{2} \int_{\Omega_j} (c_j - f)^2 dx + R_j,$$

where the residue term  $R_j = R_j[Q \setminus \{c_j\}]$  does not involve  $c_j$ . Thus,

$$F[Q] = \int_{\Gamma_j^+} (u_j^+ - c_j) ds + \int_{\Gamma_j^-} (c_j - u_j^-) ds + \frac{\lambda}{2} \int_{\Omega_j} (c_j - f)^2 dx + R_j \quad (24)$$

where  $u_j^\pm(x)$  along  $\Gamma_j^\pm$  are defined by:  $u_j^\pm(x) = \lim_{\epsilon \rightarrow 0^+} u(x + \epsilon\vec{\nu})$  a.e. for  $x \in \Gamma_j$ . Since  $\Omega_j = u^{-1}(c_j)$ , we conclude that  $u_j^\pm \in Q \setminus \{c_j\}$ . Then (24) gives,

$$\frac{\partial F}{\partial c_j} = - \int_{\Gamma_j^+} ds + \int_{\Gamma_j^-} ds + \lambda \int_{\Omega_j} (c_j - f), \quad \text{for } j = 0, 1, \dots, k.$$

Since optimality requires that  $\frac{\partial F[Q^*]}{\partial c_j} = 0$  for  $j = 0, 1, \dots, k$ , one must have

$$\lambda \int_{\Omega_j} (c_j^* - f) - (\mathcal{H}^1(\Gamma_j^+) - \mathcal{H}^1(\Gamma_j^-)) = 0, \quad j = 0, 1, \dots, k,$$

which gives  $\{c_i\}$  in (23) and completes the proof.  $\square$

The expression in (23) gives the exact updating formula for photometric optimization  $\{c_i\}$  in the AM algorithm. However, there are two main challenges for computing (23): (i) to efficiently extract the boundaries  $\Gamma_j^+$  and  $\Gamma_j^-$ , and (ii) to robustly compute  $\mathcal{H}^1(\Gamma_j^+)$  and  $\mathcal{H}^1(\Gamma_j^-)$ . Parametric approaches are notoriously clumsy in image processing and computer vision. We propose the following *region-based* algorithm for computing  $c_j$  (**P-step**):

Let  $u^n$  be the computed image at step  $n$  partitioned by  $\{\Omega_j\}$ . For each  $j = 0, 1, \dots, k$ , we perform the following.

- Define  $\Omega_j = u^{-1}(c_j)$ ,  $\Omega_j^+ = \{x \mid u(x) > c_j\}$ , and  $\Omega_j^- = \{x \mid u(x) < c_j\}$ .
- Define the smoothen versions of the characteristic functions to be  $\xi(x) = \text{smooth}(1_{\Omega_j^+}(x))$  and  $\eta = \text{smooth}(1_{\Omega_j^-}(x))$ . (Smoothing is for robust numerical computation of gradients, and can be carried out by moderate heat diffusion.)
- Let  $\Omega_j^\epsilon$  be an  $\epsilon$ -extension of  $\Omega_j$ .
- Then, we employ the following approximations:

$$H^1(\Gamma_j^+) \simeq \int_{\Omega_j^\epsilon} |\nabla \xi|, \quad H^1(\Gamma_j^-) \simeq \int_{\Omega_j^\epsilon} |\nabla \eta|. \quad (25)$$

Such region based computational scheme is often more robust than those based on parametric curve representation. Numerical examples are presented in the following section.

## 5 Computational Results and Applications

We present several computational examples and applications of the proposed quantum TV model (3) (either with a given quanta set  $Q$  or without) and the associated algorithms developed in Section 3.

Figure 2 compares quantum TV model with the simple scheme of nearest rounding of values. The image is moderately noisy in (a), and the quanta set is preassigned:  $Q = \{0, 1/3, 2/3, 1\}$ . It is evident from the example that the quantum TV model (3) excels in producing consistent geometric regularity for the quantized patches.

Figure 3 is another application of quantum TV in bar code processing. Since the gray values of the corrupted bar code image (in (a) mostly stay above zero (black), we have empirically adopted the quanta set  $Q = \{0.45, 1\}$  for the quantum TV model. The binary output is then rescaled to the canonical black-white

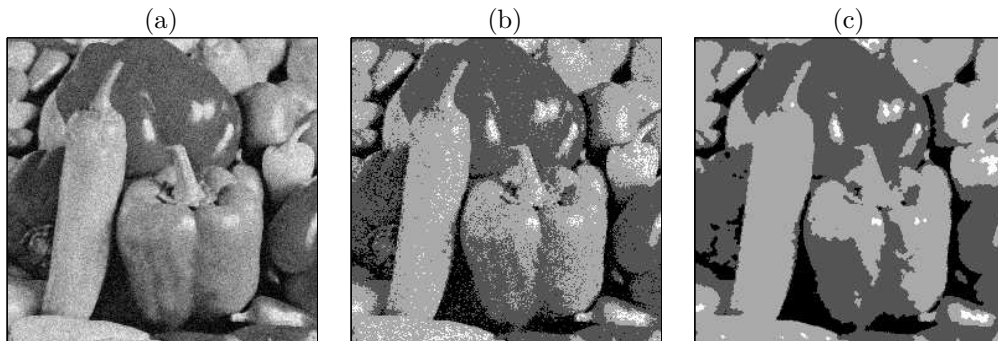


Figure 2: Comparison with simple rounding (with  $Q = \{0, 1/3, 2/3, 1\}$ ): (a) moderately noisy original image; (b) pixelwise direct rounding to the quanta set  $Q$ ; and (c) output from the quantum TV model.



Figure 3: *Bar code processing: (a) noisy and moderately corrupted bar code image; (b) output from the quantum TV model.*

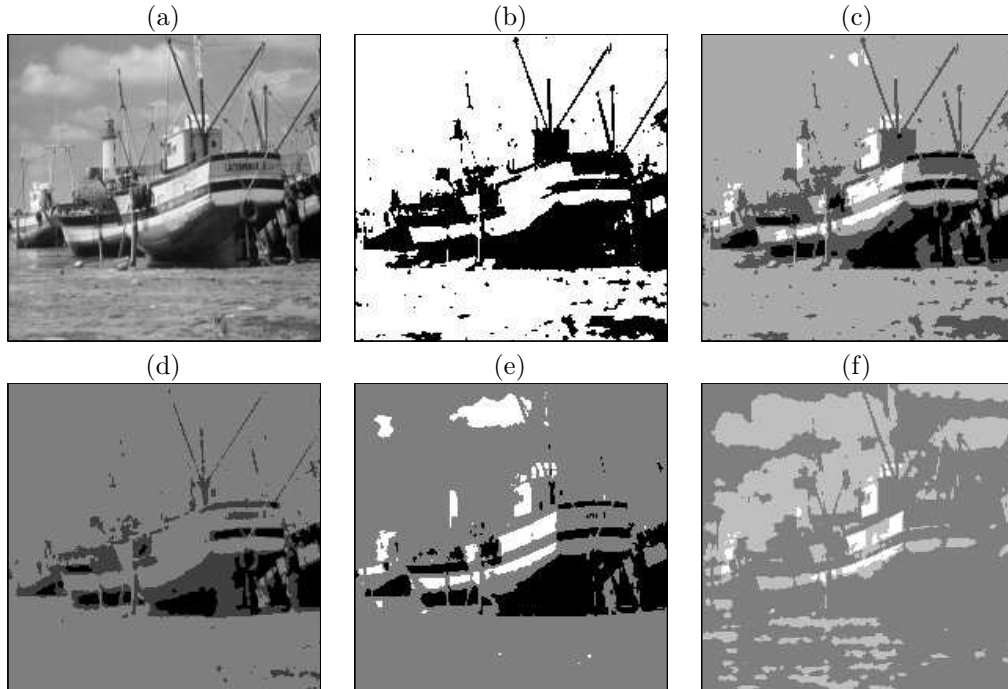


Figure 4: *Effects of different quanta sets for the quantum TV model (3): (a) original image; (b)  $Q = \{0, 1\}$ ; (c)  $Q = \{0, 1/3, 2/3, 1\}$ ; (d)  $Q = \{0, 0.25, 0.5\}$ ; (e)  $Q = \{0, 0.5, 1\}$ ; and (f)  $Q = \{0.5, 0.75, 1\}$ .*

bar code quanta  $\{0, 1\}$  (as shown in (b)). Pay attention to how the color inhomogeneity in the originally imperfect bar code image has been properly got rid of.

Figure 4 demonstrates the effect of image quantization for the “Boat” test image. Different representative quanta sets are tested (from (b) to (f)) on the original image in (a). This example partially shows the limitation of the quantum TV model with a *fixed* quanta set. In practice, different choices may lead to very different quantization outputs. Thus the example well motivates the *free* quantum TV model for which the quanta set  $Q$  is also to be optimized instead of being preassigned.

The next three examples demonstrate the performance of the *free* quantum TV model (4) and the associated two-step AM algorithm proposed in Section 4. The quanta set  $Q$  is also to be optimized with only the cardinality  $|Q| = k + 1$  information available.

Figure 5 shows an application in segmenting a noisy brain image. Based on the three clusters in the

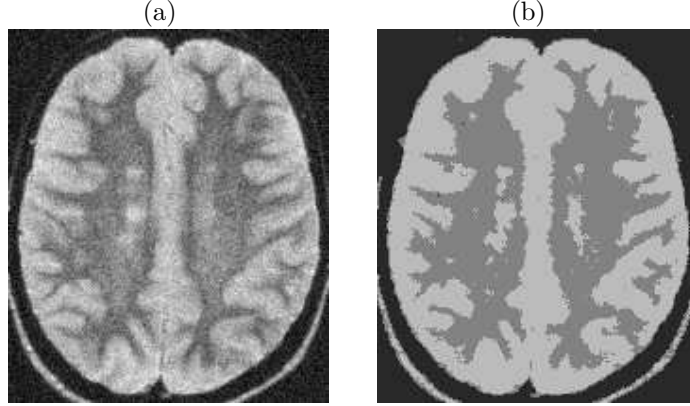


Figure 5: *Segmentation via the free quantum TV model: (a) original noisy brain image; (b) segmentation output from the free quantum TV model with  $|Q| = 3$ .*

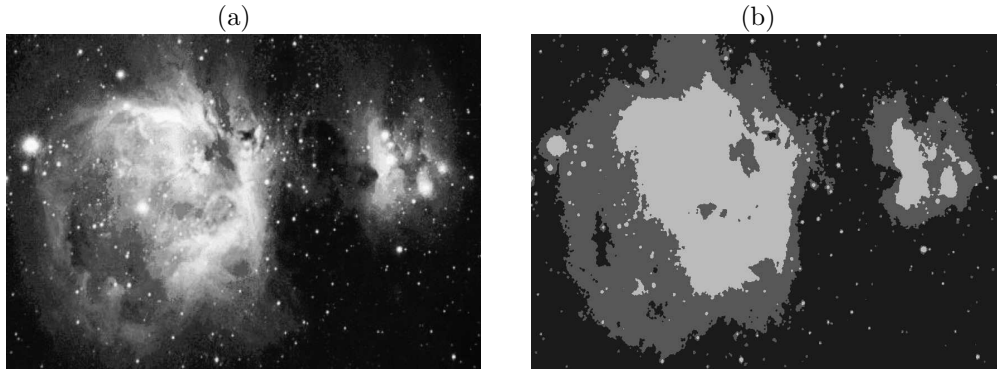


Figure 6: *Segmenting a galaxy image via the free quantum TV model: (a) original image with two nebulae; (b) segmentation by the free quantum TV model (with  $|Q| = 3$ ). The performance is comparable to the piecewise constant Mumford-Shah model.*

histogram of the given noisy image in (a), we assign  $|Q| = 3$ . The 2-step AM algorithm starts with a random initial guess for  $Q$ , and robustly converges to the optimal quanta set  $Q_* = \{0.1608, 0.5164, 0.7362\}$ .

Figure 6 demonstrates another example of image segmentation by the free quantum TV model. For this real and complex galaxy image, the performance is very comparable to the piecewise constant Mumford-Shah model and its level set implementation studied by several authors [8, 9, 13, 15, 23].

Finally in Figure 7, we demonstrate (via the Lenna image) the quantization performance of the free quantum TV model with  $|Q| = 5$  and  $|Q| = 8$ . For  $|Q| = 5$ , the quanta set  $Q$  converges to  $Q = \{0.2192, 0.3876, 0.5216, 0.6384, 0.8049\}$  (in (b1)). For  $k = 8$ , it converges to  $Q = \{0.2176, 0.3790, 0.4924, 0.5667, 0.6287, 0.6979, 0.7818, 0.8477\}$  (in (c1)). In each case, the output is compared with that from direct rounding to an equally spaced quanta set  $Q$  with the same cardinality (in (b2) and (c2)). The free quantum TV model clearly outperforms direct rounding in terms of geometric regularity and meaningfulness of pixel grouping.

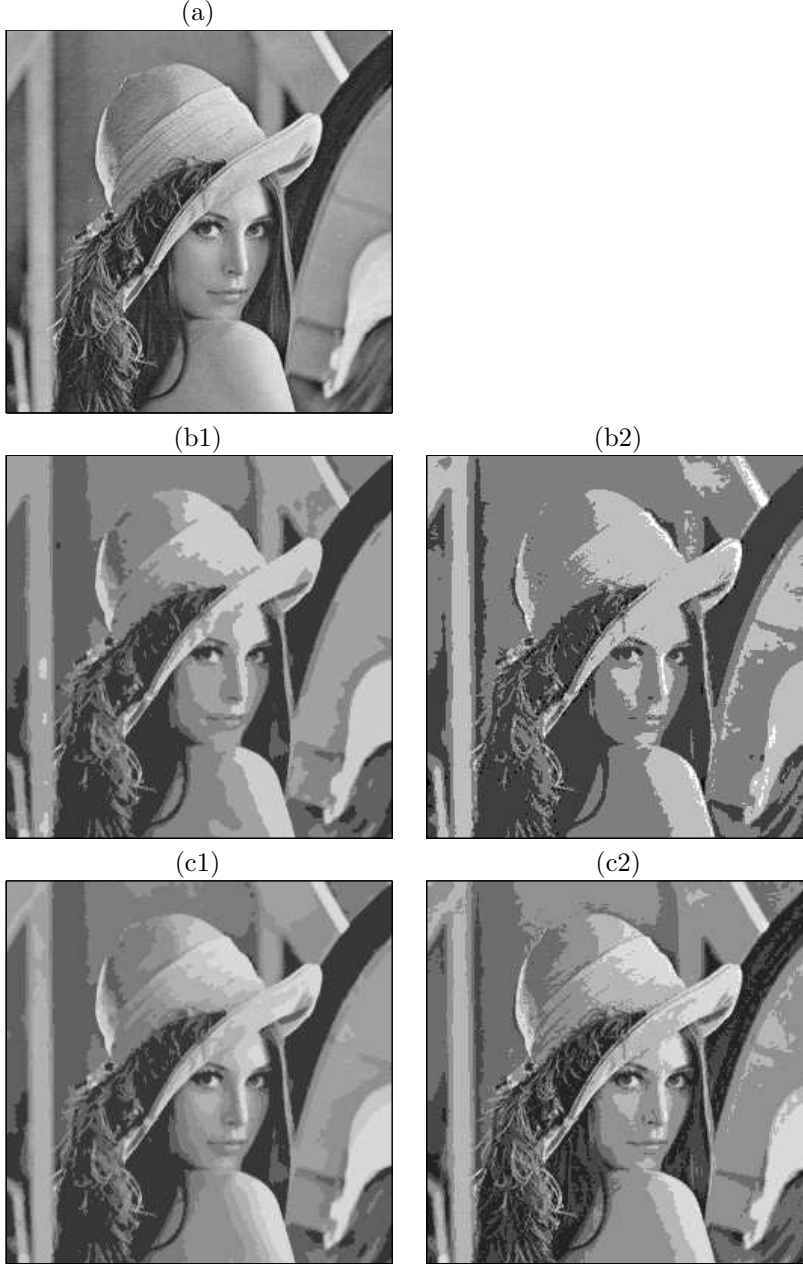


Figure 7: *Quantization via the free quantum TV model: (a) original Lenna image; (b1) quantized using  $|Q| = 5$ , with the computed optimal quanta set  $Q_* = \{0.2192, 0.3876, 0.5216, 0.6384, 0.8049\}$ ; (b2) direct rounding to an equally spaced quanta set  $Q$  with  $|Q| = 5$ ; (c1) quantized using  $|Q| = 8$ ; (c2) direct rounding to an equally spaced quanta set  $Q$  with  $|Q| = 8$ . Notice the superb performance of the free quantum TV model in terms of geometric regularity and smoothness (e.g., the facial area).*

## 6 Concluding Remarks and Discussion

In this paper, we have proposed both the quantum TV model (3) and the free quantum TV model(4), studied their mathematical properties, and developed the associated computational algorithms. Compared

with the classical TV model, the quantum TV model is more challenging due to its discrete programming nature. The models and their algorithms have been tested in several major applications in contemporary image processing, including bar code scanning, image quantization, and image segmentation.

## Acknowledgments

The authors would like to thank Professors Stan Osher and Tony Chan for their constant teaching, advising, and encouragement throughout the years. Both authors are also deeply grateful to Professor Riccardo March for his personal friendship and generous support.

## References

- [1] R. Acar and C. R. Vogel. Analysis of total variation penalty methods for ill-posed problems. *Inverse Prob.*, 10:1217–1229, 1994.
- [2] J-F. Aujol, G. Aubert, L. Blanc-Féraud, and A. Chambolle. Image decomposition into a bounded variation component and an oscillating component. *Journal of Mathematical Imaging and Vision*, 22(1):71–88, January 2005.
- [3] J.-F. Aujol and S. H. Kang. Color image decomposition and restoration. *Journal of Visual Communication and Image Representation (to appear)*, 2005.
- [4] P. Blomgren, T.F. Chan, P. Mulet, and C.K. Wong. Total variation image restoration: numerical methods and extensions. *Proc. of IEEE Int. conf on Image Processing*, 3:384–387, 1997.
- [5] A. Chambolle and P. L. Lions. Image recovery via Total Variational minimization and related problems. *Numer. Math.*, 76:167–188, 1997.
- [6] T. F. Chan, S. H. Kang, and J. Shen. Total variation denoising and enhancement of color images based on the CB and HSV color models. *J. Visual Comm. Image Rep.*, 12(4):422–435, 2001.
- [7] T. F. Chan, S. Osher, and J. Shen. The digital TV filter and nonlinear denoising. *IEEE Trans. Image Process.*, 10(2):231–241, 2001.
- [8] T. F. Chan and L. A. Vese. Active contours without edges. *IEEE Trans. on Image Process.*, 10(2):266–277, 2001.
- [9] J. T. Chung and L. A. Vese. Image segmentation using a multilayer level-set approach. *UCLA CAM Report 03-53*, 2003.
- [10] S. Esedoglu. Blind deconvolution of bar code signals. *Inverse Problems*, 20:121–135, 2004.
- [11] F. Gibou and R. Fedkiw. Fast hybrid k-means level set algorithm for segmentation. *proc. of the 4th Annual Hawaii Int. Conf. on Stat. and Math.*, 2002.
- [12] E. Joseph and T. Pavlidis. Bar code waveform recognition using peak locations. *IEEE Trans. Pattern Anal. Mach. Intell.*, 16:630–640, 1994.
- [13] Y. M. Jung, S. H. Kang, and J. Shen. Multiphase image segmentation via modica-mortola phase transition. *SIAM Applied Math.*, 2007.
- [14] S. Levine, Y. Chen, and J. Stanich. Image restoration via nonstandard diffusion. *Technical Report , Dept of Math and CS, Duquesne University*, 04-01, 2004.
- [15] J. Lie, M. Lysaker, and X.-C. Tai. A variant of the level set method and applications to image segmentation. *Math. Comp.*, 75:1155–1174, 2006.

- [16] Y. Meyer. *Oscillating Patterns in Image Processing and Nonlinear Evolution Equations*, volume 22 of *University Lecture Series*. AMS, Providence, 2001.
- [17] D. Mumford and J. Shah. Optimal approximations by piecewise smooth functions and associated variational problems. *Comm. Pure Appl. Math.*, 42(5):577–685, 1989.
- [18] S. Osher, A. Sole, and L. Vese. Image decomposition and restoration using total variation minimization and the  $H^{-1}$  norm. *SIAM multiscale Model. Simul.*, 1(3):349–370, 2003.
- [19] L. Rudin, S. Osher, and E. Fatemi. Nonlinear total variation based noise removal algorithms. *Physica D*, 60:259–268, 1992.
- [20] S. J. Shellhammer, D. P. Goren, and T. Pavlidis. Novel signal-processing techniques in bar code scanning. *IEEE Robot. Autom. Mag.*, 6:57–65, 1999.
- [21] J. Shen. On the foundations of vision modeling I. Weber’s law and Weberized TV restoration. *Physica D*, 175:241–251, 2003.
- [22] B. Song and T. F. Chan. A fast algorithm for level set based optimization. *UCLA CAM reports*, 02-68, 2002.
- [23] X.-C. Tai and Tony Chan. A survey on multiple level set methods with applications for identifying piecewise constant functions. *International J. Numer. Anal. Modelling*, 1(1):25–48, 2004.
- [24] L. Vese. A study in the BV space of a denoising-deblurring variational problem. *Appl. Math. Optim.*, 44(2):131–161, 2001.
- [25] L. Vese and S. Osher. Modeling textures with total variation minimization and oscillating patterns in image processing. *Journal of Scientific Computing*, 19(1-3):553–572, 2003.
- [26] L. Vese and S. Osher. Image denoising and decomposition with total variation minimization and oscillatory functions. *Journal of Mathematical Imaging and Vision*, 20:7–18, 2004.
- [27] C. Vogel. *Computational Methods for Inverse Problems*. SIAM, Philadelphia, 2002.
- [28] J. Weickert. *Anisotropic Diffusion in Image Processing*. Teubner-Verlag, Stuttgart, Germany, 1998.